doi:10.15625/2525-2518/22501



# Surface modification of waste gypsum for use as additive filler of greencomposites based on poly(butylene adipate terephthalate)

Do Van Cong<sup>1</sup>, Mai Duc Huynh<sup>1</sup>, Nguyen Huu Dat<sup>1</sup>, Nguyen Quang Minh<sup>1</sup>, Tran Huu Trung<sup>1</sup>, Nguyen Thi Thu Trang<sup>1</sup>, Kieu Thi Quynh Hoa<sup>2</sup>, Nguyen Vu Giang<sup>1,3,\*</sup>

<sup>1</sup>Institute for Tropical Technology, VAST, 18 Hoang Quoc Viet, Cau Giay, Ha Noi, Viet Nam
<sup>2</sup>Institute Institute of Biotechnology, VAST, 18 Hoang Quoc Viet, Cau Giay, Ha Noi, Viet Nam
<sup>3</sup>Graduate University of Science and Technology, VAST, 18 Hoang Quoc Viet, Cau Giay, Ha Noi, Viet Nam

\*Emails: vgiang@ims.vast.ac.vn; vugiang.lit@gmail.com

Received: 4 March 2025; Accepted for publication: 20 June 2025

**Abstract.** Using fillers to reinforce and improve the desired properties of polymer composite materials is the desire of researchers. In which, the dispersion ability, interaction and adhesion between fillers and polymer matrix are the key to determine the properties of the obtained materials. This study focuses on surface modification of waste gypsum particles with ethylene bis stearamide (EBS) to use it as a reinforcing filler for polybutylene adipate terephthalate (PBAT), a biodegradable polymer with many advantages such as high flexibility and good barrier properties. Using energy dispersive X-ray spectroscopy (EDX), thermogravimetric analysis (TGA) and scanning electron microscopy (SEM) images observation confirmed that the WGS granules were successfully modified with the suitable EBS content of 5 wt.%. Thanks to the modification, the processability, dispersion and adhesion of WGS to the PBAT matrix were improved, as results, the mechanical and thermal performances as well as hydrolytic resistance of obtained green composites was also enhanced.

Keywords: Polybutylene adipate terephthalate (PBAT), waste gypsum, ethylene bis stearamide, green composites, hydrolysis.

Classification numbers: 2.3.1, 2.5.1, 2.5.3, 2.9.3, 2.9.4.

# 1. INTRODUCTION

Synthetic polymers from petroleum fossil fuels have been used as materials of the 20<sup>th</sup> century and will continue to play a major role in the early 21<sup>st</sup> century thanks to their outstanding advantages such as light weight, diverse mechanical properties, various geometric conformability, sound insulation, electrical and thermal insulation, low corrosion and low cost

[1, 2]. However, due to the increasingly depleted petroleum resources and the serious environmental pollution caused by plastic waste, the findings for alternative materials for them is of great interest. In particular, natural polymers and biodegradable polymers are increasingly being prioritized [3, 4]. Biodegradable polymers can be derived from cellulose and starch, or from petroleum resource. Polybutylene adipate terephthalate (PBAT) is produced from renewable resources such as sugarcane and corn starch and is a copolyester of 1,4-butanediol, adipic acid and terephthalate acid. It is known as excellent biodegradability, which reduces its impact on the ecosystem. PBAT resin can be processed using conventional plastic processing techniques. Overall, PBAT has high flexibility and good barrier properties, which makes it a versatile material for a wide range of applications, including food packaging, agricultural films, biodegradable shopping bags, fast food packaging, and cereal containing boxes [5]. It is also used in the personal and household care products such as shampoo bottles, soap dispensers, and toothbrushes. In the medical products, PBAT is used as suture materials, wound dressings, and other medical devices. However, PBAT also has some disadvantages such as high production cost and too flexibility, which limits its applications. These disadvantages could be overcome by the combination of PBAT with other polymers or low-cost fillers, e.g., natural fibers and common minerals [6 - 8].

Gypsum has long been known to have many important applications in life, from construction to medicine, art... Gypsum is mainly known as natural gypsum, the main chemical component is calcium sulfate, an inorganic compound with the molecular formula  $CaSO_4.2H_2O$ . It is a white, gray or brown solid, hardness of about 2 - 2.5 on the Mohr hardness scale and insoluble in water. It is also one of the commonly used fillers for many types of thermoplastics due to its many good properties such as chemical resistance, heat resistance, good fire resistance, especially low cost. Another advantage is that due to its high density, gypsum is used in the manufacture of polymer composite materials to reduce shrinkage, improve tensile or impact resistance and improve the gloss of the material [9,10].

Waste gypsum (WGS), a by-product of the process of producing nitrogen fertilizer from apatite ore, contains the main chemical components such as 48 % CaSO<sub>4</sub>.2H<sub>2</sub>O, 21.64 % Ca(OH)<sub>2</sub>, 14.8 % CaCO<sub>3</sub>, 5.82 % CaO, 4.31 % SiO<sub>2</sub>, and other metal oxides [11]. With a large residual acid content and huge residues, WGS has the high risk of polluting the environment and water sources around the dumps [12]. Therefore, the effective treatment and utilization of WGS not only solves environmental problems but also helps to effectively utilize these raw materials [13]. Similar to gypsum, WGS has high heat resistance, fire resistance, abrasion resistance and weather resistance, which makes the advantages as an additive for cement, concrete, construction bricks, plastics and rubbers [12]. By the treatment and surface modification, WGS could be used as a good filler for the gypsum-based polymer composites with various polymer matrix such as polypropylene, polyethylene, polyvinyl chloride, epoxy... F. Ramos et al. [10] used gypsum with contents of 50, 60 and 70 % mixed with molten recycled high-density polyethylene (HDPE). The addition of WGS increased the crystallinity degree, thermal stability and flammability of HDPE while HDPE acted as waterproofing of gypsum. Yordan D. Denev et al. introduced 10 to 60 wt.% phosphogypsum (PG) into polyethylene at melting state to obtain the composite owning high tensile strength and modulus strength [14]. High-density polyethylene (HDPE)/phosphogypsum (PG) and polypropylene (PP)/PG composites were also fabricated by using a twin screw extruder. The presence of PG improves the thermal stability and increased significantly the Young's modulus and tensile strength composites, but decreased remarkably the impact strength and elongation at break of obtained composites [15]. M. Doleželová indicated that WGS improved water resistance of epoxy resin [16]. In previous work, we also conducted the combination of WGS with various thermoplastics such as HDPE/EVA blend [17], HDPE [18], PP [19], polyvinylchloride (PVC) [20]. The experimental results showed that the incorporation of WGS improved the processability, mechanical properties, thermal properties and fire resistance of these composites.

With many efforts to create the green composite materials, blending WGS with some biodegradable polymers has been conducted. M. Murariu et al. [21] have successfully manufactured a polylactic acid (PLA)/gypsum material system using a plasticizer. The presence of the plasticizer has improved the processability, increased the impact strength and dispersibility of gypsum on the PLA matrix. In previous our work, we used ethylene bis stearamide (EBS) as a surface modifier for WGS before dispersing into molten PLA. With the introduction of 25% modified WGS, the Young's modulus, tensile strength, and flexural strength of biocomposites increased respective to 92.6; 37.3; and 13.3; 8.3 % as compared to modified samples [22]. Recently, some preliminary studies on PBAT/gypsum composites have appeared. T. W. Kong et al. used stearic acid (SA), polyethylene glycol (PEG), and malic acid (MA) to modify the surface of waste gypsum to address them into PBAT [23,24]. The MA-treated gypsum (MA-gypsum) showed the best performance, whereas SA-gypsum showed the worst performance in the mechanical properties of obtained composites due to the presence of both -OH and -COOH groups in MA, which is responsible for the superior surface treatment of gypsum and its better dispersion in the polymer matrix [23]. Compared to calcium carbonate, gypsum is more polarizable due to owning larger anion  $SO_4^{2-}$  and  $CaCO_3$  is more ionic whereas. Hence, the dispersibility of gypsum in the PBAT matrix better than CaCO<sub>3</sub> [24]. However, the number of studies on this material is still quite limited.

As known, the performances of polymer composites much depend by the dispersion, interaction, and the interfacial adhesion between the filler and the polymer matrix [25-28]. Therefore, the surface modification of waste gypsum (WGS) has been carried out with various organic compounds such as stearic acid, sodium dodecyl sulfate (SDS), malic acid, polyethylene glycol (PEG), and malic acid (MA) before being mixed with the polymer. Ethylene bis stearamide (EBS) was used for the surface modification of WGS in some previous works. There, the presence of EBS was demonstrated through FTIR spectra and the surface modification with EBS significantly improved the processability, dispersion and adhesion between WGS and the polymer matrix, thereby improving some mechanical properties and thermal stability for the composites [17,18,22]. However, the information on this modification still quite limited, and EBS coating and/or grafting efficiency, the structural morphology before and after modification as well as and the dispersion ability of the microparticles have not been mentioned.

Continuing to study this direction further, this study conducted some investigations on the surface modification of WGS and the effects of EBS modified WGS on the processability, structure morphology, mechanical and thermal stabilities as well as the hydrolysis of PBAT/WGS green composite materials.

# 2. MATERIALS AND METHODS

### 2.1. Materials

Polybutylene adipate terephthalate (PBAT), commercial named @KB100, is produced by polycondensation reaction, consisting of a copolyester of 1,4-butanediol, adipic acid and terephthalate acid; white granulates with specific gravity 1.22 g/cm³, melting point 115 - 125 °C, melt flow rate MFR 3.0 - 5.0 (g/10min, 190 °C 2.16 kg) and supplied by Zhuhai Kingfa Biomaterial Co., Ltd. (China). WGS was taken from the waste dump at DAP Vinachem

Company, Dinh Vu Industrial Park, Hai Phong, Vietnam. Ethylene bis stearamide (EBS) in superfine form is a commercial product of Merck Company, with a purity of 99.8 %.

# 2.2. Waste gypsum treatment and modification

Waste gypsum treatment: Waste gypsum (WGS), from Dinh Vu DAP factory, was precrushed, sieved with a sieve with a diameter of 125 micrometers to remove large particles and impurities. This obtained WGS is called original WGS granules, which is denoted as o-WGS. Next, o-WGS is washed with water several times and the residual acid is neutralized with lime water solution to neutral pH. Then, the gypsum is filtered, washed and dried for 12 hours at 110 °C. After drying, the gypsum is crushed and sieved once again to obtain treated WGS granules, which is denoted as t-WGS.

Surface modification of WGS: The surface modification of t-WGS with EBS was described in some the previous work [17,18,22]. Briefly, t-WGS granules were premixed with 6 wt.% EBS (compared to the mass of t-WGS), then the mixture was heated to 170 °C and kept for 15 minutes. During this time, EBS melted and then the surface of t-WGS was coated or impregnated with EBS. The residual EBS was removed by Soxhlet with a mixture of ethanol: water = 1:1 and finally, the modified gypsum (denoted as m-WGS) at 80 °C in a vacuum oven until the constant mass.

### 2.3. Fabrication of PBAT/gypsum green composites

The mixtures of PBAT and original and/or modified WGS with the predetermined weight ratios were melt mixed in the Haake Polylab OS Rheodrive 7 under 140 °C for 5 minutes with the rotor speed kept at 50 rpm. The filling coefficient for the mixing chamber was 0.8. After finishing the mixing, the molten sample was taken out and transferred into the Toyoseiki instrument to be pressed into a flat sheet. Herein, this instrument was preheated at 140 °C and the pressing pressure was 5 MPa. The sample after fabrication was kept at room temperature for at least 24 hours before the characterization.

# 2.4. Characterizations

- Structural morphology analysis: Using scanning electron microscopy (SEM) images to evaluate the changes in surface structure morphology of WGS before and after being treated and modified with EBS as well as the changes in structural morphology of composites. SEM measurements were captured by a JMS-6510LV device from Jeol (Japan).
- Energy dispersive X-ray spectroscopy (EDS or EDX): This measurement was conducted by the combination with JSM- 6510LV instrument, using X-ray energy scattering probe, Oxford Instruments (UK) to determine the distribution and elemental composition of materials. The electron acceleration voltage was applied at 15~kV and the sample surfaces were coated with platinum before testing.
- Thermogravimetric analysis (TGA): Thermogravimetry (TG) and derivative thermogravimetry (DTG) was performed on a TGA 209F thermogravimetric analyzer, Nezsch (Germany) with a heating rate of  $10\,^{\circ}$ C/min, air environment, from  $25-600\,^{\circ}$ C.
- Melt rheology properties: The experiment was conducted on a Thermo scientific (USA) melt rheometer model Haake Polylab OS RheoDrive 7 with a closed mixing chamber, using two rollers of mixing shafts according to ASTM D 2538 standard.

- Tensile properties: The tensile strength, elongation and Young's modulus parameters of the samples were performed on a Zwick Z2.5 instrument (Germany) at room temperature with a tensile speed of 50 mm/min, according to ASTM D638 standard. Each type of sample was determined at least 3 times to get the average values.
- Alkaline hydrolysis resistance: The hydrolysis of PBAT and composites was tested by immersing  $20 \times 20 \times 1~\text{mm}^3$  samples in 50 mL of NaOH  $10^{-2}$  M aqueous solution (4 g/L). After interval time, the samples were removed and washed with deionized water, then dried with paper, and finally dried in a vacuum oven at 60 °C for 24 h. The hydrolysis was preliminarily evaluated based on the weight loss over the immersion time and the SEM images of the samples. The weight loss was calculated according to the following formula:

Weight loss = 
$$\frac{w_0 - w_t}{w_0} \times 100 \tag{1}$$

where,  $w_0$  and  $w_t$  is respective to the initial weight of the specimen and the weight of the specimen after drying at immersing time t.

### 3. RESULTS AND DISCUSSION

### 3.1. Surface modification of waste gypsum by EBS

In this study, the improvement in the dispersion of WGS can be observed in Figure 1. With the same weight dispersed in the same volume of ethanol and after 10 minutes of dispersion, it can be seen that the o-WGS and the treated WGS had an obviously separation, the clearer solution layer was on top and the precipitate layer gradually formed at the bottom of the glass vial. Reversely, the WGS samples treated and modified with EBS (m-WGS) were still very turbid with a fairly uniform color, and the formation of a precipitate layer at the bottom of the vial was not observed yet.

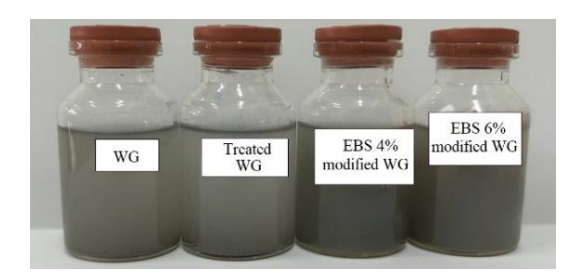


Figure 1. Dispersion in ethanol of WGS granules before and after treatment and modification with EBS recorded after 10 minutes.

EDX analysis showed that the original sample had a fairly high organic content with an initial C content of 14.6 wt.%. In addition, some elements mixed in the ore also appeared such as Si, K, Al, F. After treatment and washing, these elements were almost removed. At the same time, the C content decreased to 8.1 %; proving that the organic content was partially removed. Thanks to that, the purity of CaSO<sub>4</sub> increased, with the weight percentage of Ca element changed from 14.3 % to 21.1%. It is noteworthy that for the modified WGS sample, the carbon content increased from 8.1 to 13.3 wt%. This showed that EBS was present on the modified WGS particle. However, the characteristic peak of the N element in the amide group, which usually appears at 0.38 - 0.4 keV, was absent in the EDX spectrum, possibly due to overlap in the peak of the O element (Figure 2).

The EBS content coated on the surface of WGS granules can be determined by TGA. Figure 3a displayed the TGA and DTG diagrams showing that the weight loss of o-WGS happened through mainly one stage from room temperature to 160 °C with a weight loss of 6.87 % due to the evaporation of absorbed moisture and the dehydration reaction of gypsum as shown in the reaction 2. The second stage was without the peak on DTG but appeared unobvious on TGA diagram in the range from 200 °C to 700 °C with a very small mass loss (1.14 %). It may be due to the release of the complete decomposition of impurities and was mainly caused by the dehydration of gypsum when it converted into anhydrite as following:

$$CaSO_4.2H_2O \rightarrow CaSO_4.0.5 H_2O + 1.5 H_2O (at 150 \,^{\circ}C)$$
 (2)

$$CaSO_4.1/2H_2O \rightarrow CaSO_4 + 0.5 H_2O (> 150 °C)$$
 (3)

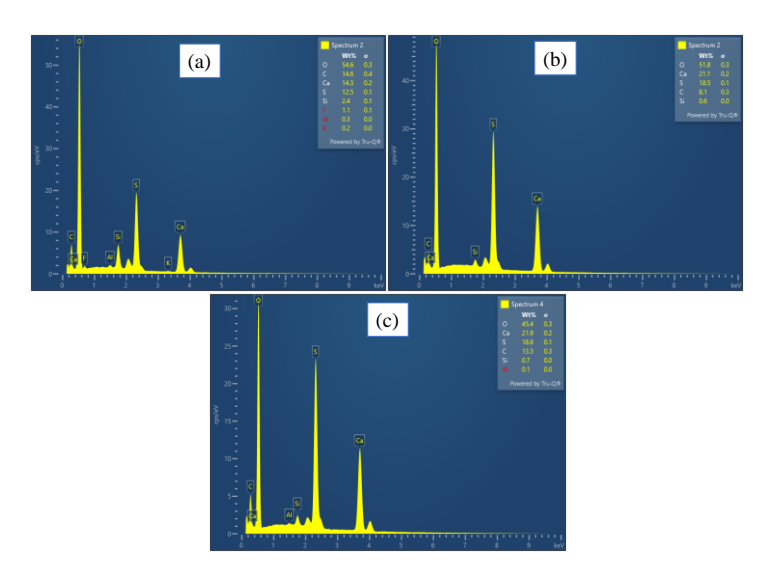


Figure 2. EDX patterns of the original (a), treated (b) and EBS-treated and modified (c) waste gypsum samples.

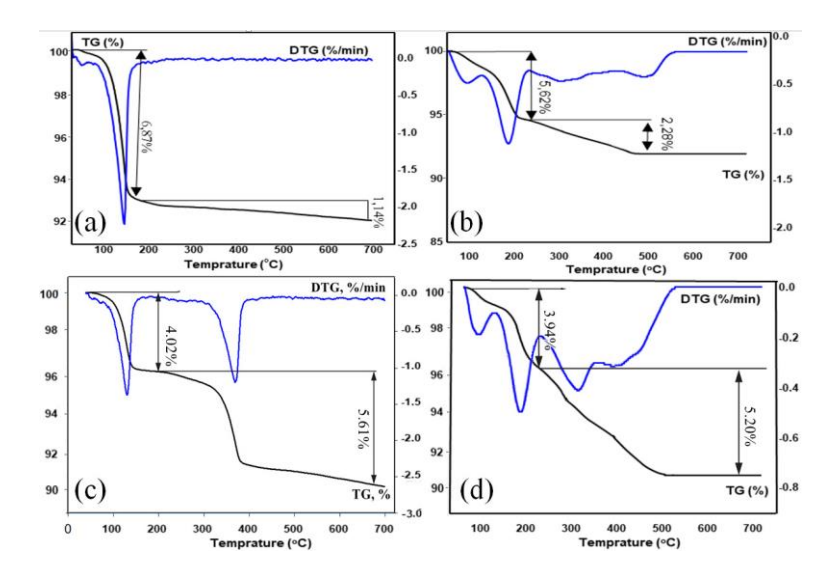
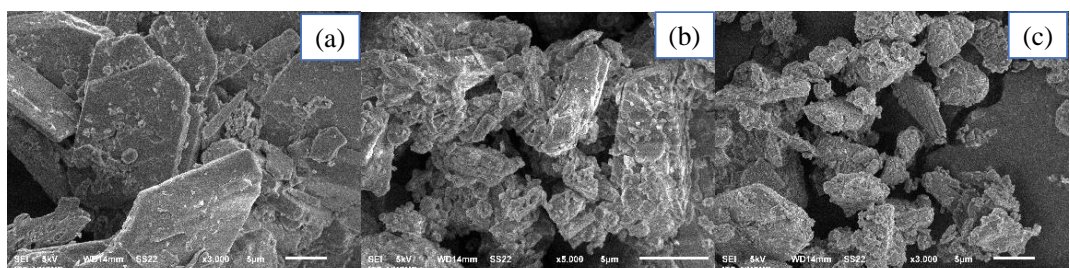


Figure 3. TG and DTG diagrams of (a) o-WGS and WGS modified with (b) 3 wt%, (c) 5 wt%, and (d) 7 wt% EBS.

In the presence of EBS as a modifier, the weight loss of m-WGS occurred in the two or three stages (Figures 3b, c and d). The first stage (below 200 °C) was assigned to the dehydration of gypsum as being calcined with the fewer weight loss compared to o-WGS. This was caused by two main reasons: first, the modification process occurred at 170 °C, where the dehydration happened partly following the reaction 2. Secondly, the modification resulted the EBS layers coated on WGS surface granules, which limited the adsorption of moisture.

From 200 °C to 600 °C, in addition to the separation of water from the conversion of gypsum to anhydrite form as the reaction 2 and 3, the weight loss at this stage was mainly due to the thermal decomposition of the organic components present in the m-WGS because almost organic compounds decomposed when calcined to 500 °C. Therefore, it can be inferred that the weight of EBS coated on the m-WGS is approximately determined as the difference between the weight loss at this stage and 1.14%, which is weight loss caused by the release of the complete decomposition of impurities and mainly the dehydration of o-WGS when converted into anhydrite according to reactions 2 and 3 as afore mentioned. Since then, it is easy to determine the EBS content and modification efficiency. With using 3, 5 and 7 wt.%, the EBS content attached onto the WGS surface was in turn 1.14%; 4.47% and 4.06%, respective to the modification efficiency reached to 38.0%; 89.4% and 58.0%. The content and efficiency of EBS coating on the WGS surface depend on the size and structure of WGS, the feeding content of EBS and especially the interaction between WGS and EBS. This interaction is mainly physical interactions and adsorption occurring at the active sites of WGS surface and polar functional groups on EBS. When the feeding EBS content is too high, the numbers of active sites were blocked and the adsorption on the EBS surface became saturated. Then, increasing the input content of EBS not only did not increase the content of EBS coated on the WGS surface but also reduced the efficiency of the coating/modification process. These results showed that the highest coating content and modification efficiency were obtained when using 5% EBS content and this content was used for the further investigation.

The structural morphology of the three types of WGS including origin, treated and modified with EBS, were observed on the SEM images in Figure 4. Figure 4a indicated that the o-WGS granules consisted of crystalline plates or lamellas with sizes ranging from 10 to 20  $\mu m$  stacked on top of each other and had a fairly smooth surface. After being treated and crushed, WGS were separated into the smaller plates or lamellas with the sizes ranging from sub-micro to about 4  $\mu m$  (Figure 4b). After being modified with EBS, the WGS granules were more separated with the smaller and more uniform in size, from 5 to 10  $\mu m$ . Simultaneously, the surface of them became more porous and rougher due to the appearance of a layer of loose material, which was the EBS layer covered on the WGS surface.



Figure

4. SEM images of (a) o-WGS, (b) treated and crushed WGS, and (c) m-WGS at the same magnification of  $3000\times$ .

# 3.2. Processability and performances of WGS/PBAT green composites

### 3.2.1. Melt rheological properties

The melt rheological properties were shown through the melt torque-mixing time diagrams of PBAT and its green composites with WGS. It can be seen that the shape of the torque-mixing time diagrams of all samples was similar. The torque reached the maximum value immediately after the material mixture was loaded and the mixing chamber was closed. Under the effect of high temperature, the polymer melted and/or plasticated, causing the torque to gradually decreased and reached a stable value after 3 minutes of mixing (Figure 5). Then, the polymer completely plasticated and/or melted and mixed uniformly with WGS. After 5 minutes of mixing, PBAT had a relatively low torque value of 10.2 Nm, showing that this polymer had high flexibility. When 10 wt.% and 30 wt.% o-WGS were introduced, the steady-state torque of the mixture remained almost unchanged in comparison to PBAT, with values of 9.7 Nm and 10.3 Nm, respectively. The difference was only clearly shown when using o-WGS content up to 50 wt.%, the steady-state torque of this sample reached 15.1 Nm. That is, WGS is inorganic filler with a fairly large granules size, which can hinder the motion of polymer macromolecular chains, especially when the WGS content was larger. However, in fact, the torque values unchanged significantly until 30 wt.% o-WGS was added. This clearly proved that PBAT had good blending ability with high filler contents. More interestingly, with the modification, the torque of the composites was even significantly reduced compared to the samples using o-WGS (Figure 5b) with values of 6.6 Nm and 9.1 Nm when 10% and 30% m-WGS were added, respectively. This was due to EBS acting as a lubricant, reducing the entanglement and friction generated between the components and making the material processing easier [22].

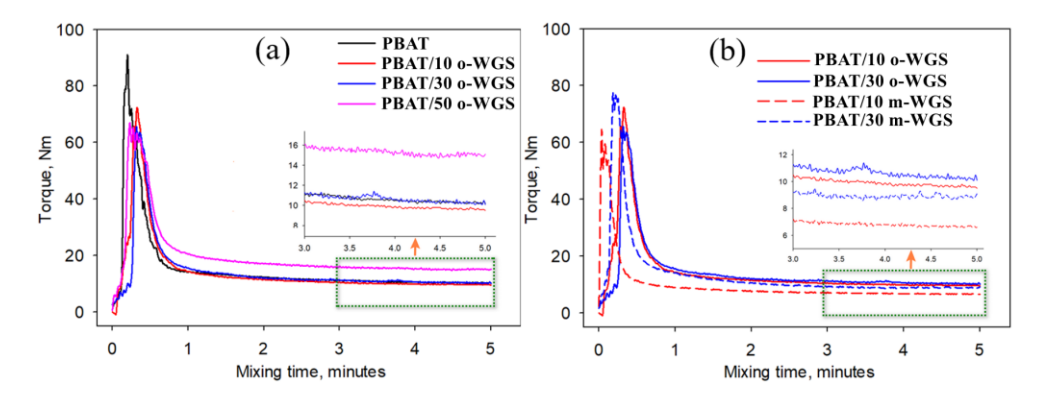


Figure 5. Melt torque-mixing time diagrams of PBAT and green composites containing various WGS content.

### 3.2.2. Mechanical properties

Table 1 exhibited the Young's modulus, elongation at break and tensile strength values of PBAT and composites. PBAT proved as a highly flexible and quite tough polymer with tensile strength 32.69 MPa and elongation at break reached up to 1265%, while the Young's modulus was quite low, only 15.32 MPa. With the introduction of WGS, both the ε and σ values of PBAT gradually decreased, while the Young's modulus gradually increased with the WGS content from 10 to 30 wt.%. However, when the WGS content increased to 40 wt.% and higher, all three above parameters showed a sudden decrease. This was probably caused by the agglomeration of WGS in the PBAT matrix. The samples using m-WGS had slightly increased mechanical strength compared to the samples containing o-WGS. It confirmed that EBS modification could

improve the mechanical strength of composites due to the better dispersion, interaction and adhesion of WGS with PBAT matrix.

<i>Table 1.</i> Young's modulus (E-Modulus), elongation at break ( $\epsilon$ ) and tensile strength ( $\sigma$ ) of PBAT and
composites containing different o-WGS and m-WGS contents.

PBAT/WGS		o-WGS			m-WGS		
weight ratios	E-Modulus, MPa	ε, %	σ, MPa	E-Modulus, MPa	ε, %	σ, MPa	
100/0	15.32	1265	32.69	-	-	-	
90/10	23.09	889	22.20	-	-	-	
80/20	28.86	759	18.88	29.23	785	19.18	
70/30	60.95	554	14.05	61.32	577	14.61	
60/40	42.65	276	8.87	42.70	310	9.43	
50/50	42.19	35	7.58	-	-	-	

### 3.2.3. Structural morphology

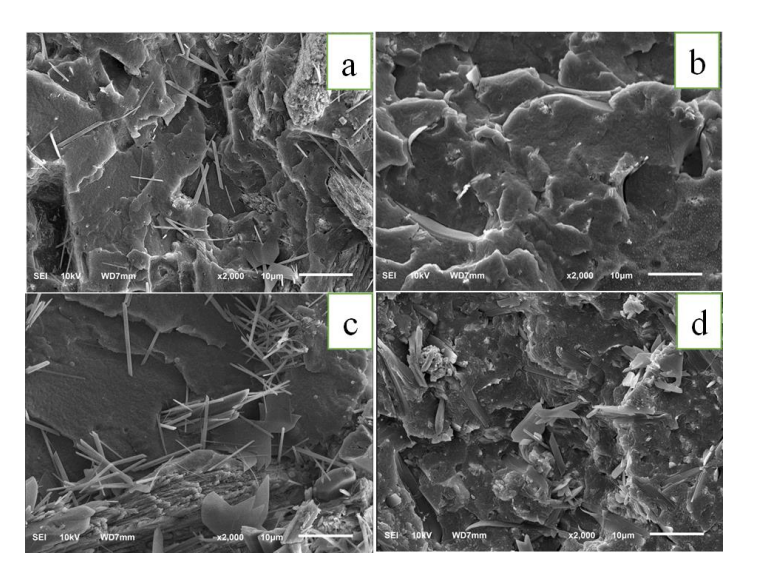


Figure 6. SEM images of the cross-sectional surfaces of green composites containing (a, b) 30 wt.% and (c, d) 40 wt.% WGS. Where, a and c were samples using o-WGS, c and d related to samples using m-WGS.

The dispersion, interaction and adhesion between WGS and PBAT matrix can be observed in the SEM images of the cross-sectional surfaces of the green composites. At lower content (30 wt.%), o-WGS existed as the long rods and slabs, about 10 to 15  $\mu$ m, distributed fairly evenly in the cross-sectional surface of the sample, however, the boundary between them and the resin matrix was quite clear (Figure 6a). Such length was because o-WGS was only treated without being crushed and modified. When the content increased to 40 wt.%, the o-WGS more locally dispersed, there was a clear clustering of WGS rods and slabs into the bundles and clumps in the PBAT matrix and the surface boundary between them and the matrix was clearly observed, even there were the appearance micropores or micro-voids around the surface of WGS (Figure 6c).

After the treatment and crushing process and especially the modification with EBS, the SEM images in Figure 6b showed the dispersion of m-WGS became more uniformly and without clear boundary between m-WGS and polymer matrix observed at the interface between the two phases. This means that the dispersion of m-WGS was improved and they adhered well to PBAT. Even when the content increased to 40 wt.%, although there was a certain local agglomeration, however, m-WGS still quite well adhered to the resin matrix and without the distinct boundary (Figure 6d). The good adhesion created a continuous structure of the composites, which helped to evenly dissipate the external force onto the material, thus improving the mechanical strength. Reversely, without being crushed and surface unmodified, the dispersion and especially the adhesion between the o-WGS and PBAT matrix were not improved, there was a clear separation between two these phases with micro-voids appeared at the interface. Thus, the external force onto the material concentrated locally, causing rapid destruction of the samples. This was clearly demonstrated by the sudden decrease in mechanical strength of the composites samples at high o-WGS contents as described above section.

### 3.2.4. Thermal stability

According to the results of tensile testing and SEM image analysis, it can be seen that the composites containing 30 % WGS have quite high elongation and tensile strength greater than 10 MPa. This material can meet the mechanical requirements in many applications. Therefore, other characteristics of this material will be studied further, such as thermal stability, chemical resistance.

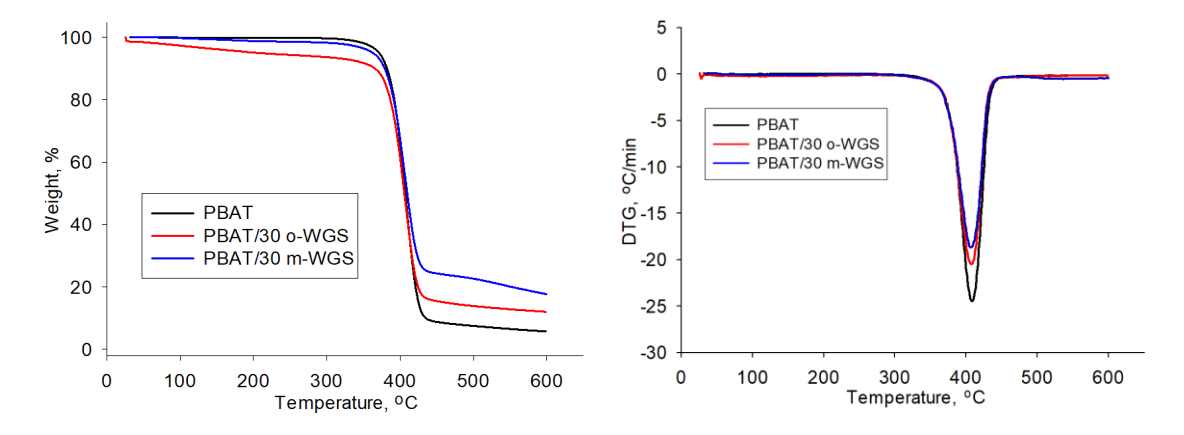


Figure 7. TG and DTG diagrams of PBAT and green composites containing 30 wt.% o-WGS (PBAT/30 o-WGS) and EBS-modified WGS (PBAT/ 30 m-WGS).

Figure 7 displayed the TG and DTG diagrams of PBAT and composites containing 30% WGS. It is observed that all above curves had similar shapes with a major weight loss found in the range from 340 to 450 °C. The sharp and strong intense peaks shown in the DTG diagrams indicating that the weight loss of PBAT and the composites occurred very quickly. The weight loss of PBAT was caused by the thermal oxidation decomposition of this polymer. While the weight loss of the composites was contributed by the evaporation of adsorbed moisture, the dehydration due to the transformation of gypsum to anhydrites beside the thermal oxidation decomposition of PBAT. This is most evident in the o-WGS composites. Due to the untreated and surface unmodified, the sample adsorbed a lot of water, causing the sample to lose the weight very early. Below 160 °C, the weight loss was about 3.4 wt.%. At the stage from 160 to

340 °C, the composites containing o-WGS continued to lose the weight due to the dehydration of gypsum into anhydrite form. Such the evaporation and dehydration formed thermally conductive microchannels and the penetration of oxygen, which could stimulate the thermal decomposition process of PBAT.

Table 2 indicated that the beginning decomposition temperature (T<sub>b</sub>) of the o-WGS composite occurred at 345.2 °C, which was earlier than that of PBAT at 347.1 °C. The maximum decomposition temperature  $(T_{max})$  and the temperatures with the same weight loss occurred were also lower than those of PBAT. All these parameters indicate that the o-WGS composites had lower thermal stability than PBAT. In contrast, with the introduction of m-WGS, the obtained m-WGS composite had higher thermal stability than PBAT and another composite, as shown by the significantly higher T<sub>b</sub>, T<sub>max</sub> and the same weight loss occurred at higher temperature compared to the other samples. This was due to three main reasons. Firstly, the EBS modification process was carried out at 170 °C, above the temperature at which the dehydration in the gypsum structure occurred as shown by the reaction (2) and (3). Secondly, with a relatively hydrophobic organic covered layer, the moisture content adsorbed on the composites was reduced, and finally, the EBS organic layers improved the dispersion, interaction and adhesion of m-WGS to the PBAT matrix. Therefore, the finer structure was resulted and retarded the decomposition of the composite materials. Moreover, the WGS lamellas with high thermal stability could play a role in heat shielding, helping to protect and prevent the thermal oxidation decomposition process of PBAT.

Table 2. TG and DTG characteristics of PBAT and its biocomposites containing 30 wt.% of o-WGS (PBAT/30 o-WGS) and m-WGS (PBAT/ 30 m-WGS)

Samples	T <sub>b</sub> , °C	T <sub>max</sub> , °C	Temperature causing the same weight loss, °C			
Samples			20 %	40 %	60 %	80 %
PBAT	347.1	408.1	392.1	403.0	411.1	421.0
PBAT/30 o-WGS	345.2	407.3	386.8	400.7	410.6	424.5
PBAT/30 m-WGS	349.6	411.7	393.6	407.6	418.2	554.7

# 3.2.5. Hydrolysis of biocomposites

Hydrolysis of PBAT and biocomposites containing 30 % WGS was performed in dilute alkaline solution (10<sup>-2</sup> M NaOH solution) to evaluate the hydrolysis resistance of these materials. Thereby, the effect of surface modification on the adhesion between m-WGS and PBAT matrix was clarified. Figure 8 showed that all material samples lost the weight and the weight loss increased gradually with immersion time. Compared with PBAT, o-WGS composites lost more much the weight under the same time conditions. On the contrary, m-WGS composites lost less the weight than the other two samples. After 9 days of immersion in 10<sup>-2</sup> M NaOH solution, the weight loss of PBAT and o-WGS and m-WGS composites was 14.85 %; 18.22 % and 8.25 %, respectively. The weight loss occurred due to during the immersion process in alkaline solution, PBAT was hydrolyzed because this is a polyester with a large number of ester functional groups. There are three different types of ester linkages within the carbon backbone of PBAT chains, meaning that hydrolysis can occur at three different positions with the different mechanisms. Q. Deshoulles et al. indicated that, the hydrolytic reaction took place on the ester located between the terephthalate and adipate groups firstly; then, for higher levels of degradation the ester situated in the adipate group would also react with water [29]. The hydrolytic reactions of PBAT were found more quickly in the presence of acid or alkaline as catalysts [30]. When being hydrolyzed continuously, the ester linkages were broken and formed the low molecular weight organic compounds, which were soluble in water, thus causing the weight loss of material.

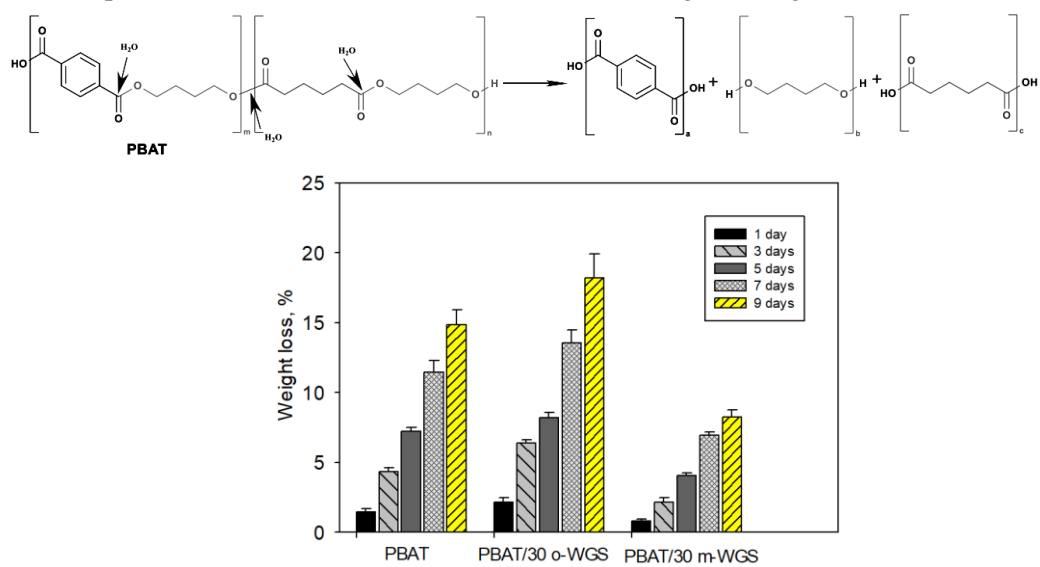


Figure 8. Weight loss of PBAT and green composites containing 30 % WGS under alkaline conditions.

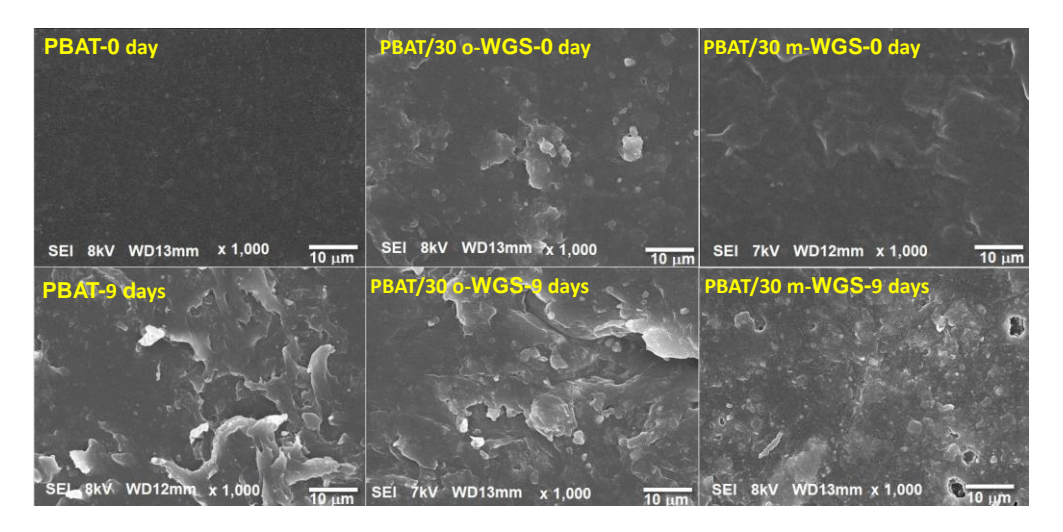


Figure 9. SEM images of the surface of PBAT and its composites before and after 7 days of immersion in  $10^{-2}$  M NaOH solution.

During the hydrolysis process, the partially separation and dissolution of soluble organic compounds, thus leading the formation of micro-voids or eroded sites. This was shown in the SEM images of the surface of PBAT and its composites before and after 7 days of immersion in  $10^{-2}$  M NaOH solution. The initial surfaces of these materials were quite smooth. After 7 days of immersion in alkaline solution, the surfaces of PBAT and o-WGS composites showed large corrosion cavities, while the density of cavities on the surfaces of m-WGS composites were quite fewer with the smaller size (Figure 9). This once again confirms that thanks to the surface modification by EBS, WGS granules interacted and adhered better with the PBAT matrix. These

interactions could be electrostatic interactions, hydrogen bonds or dipole interactions between amide and ester functional groups presenting in the material [23, 24]. This created a tight and uniform structure, thereby improving the mechanical properties, thermal stability and hydrolysis resistance of the material.

### 4. CONCLUSIONS

By changing the EBS content and using EDX, TGA and SEM analysis methods, WGS granules were successfully modified with the suitable EBS content of 5 wt.%. The EBS content attached onto the WGS surface reached 4.47 wt.% with the modification efficiency 89.40%. After being modified, an organic coating appeared on the WGS surface, thereby improving the processability, dispersion and adhesion of WGS to the PBAT matrix. Compared with the green composites using the original WGS, the green composites using the modified WGS had better mechanical strength, thermal stability and hydrolysis resistance, and even its thermal stability and hydrolysis resistance were better than PBAT. This material promises to have many potential applications and would further investigate in the near future.

*Acknowledgements.* This research was financially supported by project NCVCC13.04/24-25 of Vietnam Academy of Science and Technology.

*CRediT authorship contribution statement.* Do Van Cong: Methodology, Investigation, Manuscript preparation and editing. Mai Duc Huynh: Investigation. Nguyen Huu Dat: Formal analysis. Nguyen Quang Minh: Investigation, Formal analysis. Tran Huu Trung: Investigation. Kieu Thi Quynh Hoa: Formal analysis. Nguyen Vu Giang: Built scientific idea, Funding acquisition, Manuscript preparation and editing. All authors have read and agreed to the published version of the manuscript.

**Declaration of competing interest.** There are no conflicts to declare.

### REFERENCES

- 1. Burford R. Polymers: A historical perspective, Journal and Proceedings of the Royal Society of New South Wales, **152** (473/474) (2019) 242–250. https://search.informit.org/doi/10.3316/informit.912126913382331
- 2. Bazli L., Bazli M. A review on the mechanical properties of synthetic and natural fiber-reinforced polymer composites and their application in the transportation industry, J. Compos. Compd. **3** (9) (2021) 262–274. https://doi.org/10.52547/jcc.3.4.6
- 3. Arutyunov V. S., Lisichkin G. V. Energy resources of the 21st century: problems and forecasts. Can renewable energy sources replace fossil fuels, Russ. Chem. Rev. **86** (2017) 777. DOI 10.1070/RCR4723
- 4. Spierling S., Knüpffer E., Behnsen H., Mudersbach M., Krieg H., Springer S., Albrecht S., Herrmann C., Endres H.-J. Bio-based Plastics A review of environmental, social and economic impact assessments, J. Clean. Prod. **185** (2018) 476-491. https://doi.org/10.1016/j.jclepro.2018.03.014
- 5. Jian J., Xiangbin Z., Xianbo H. An overview on synthesis, properties and applications of poly(butylene-adipate-co-terephthalate)–PBAT, Adv. Ind. Eng. Polym. Res. **3** (1) (2020) 19-26. doi:10.1016/j.aiepr.2020.01.001
- 6. Clizia A., Massimiliano B. Addition of thermoplastic starch (TPS) to binary blends of poly (lactic acid) (PLA) with poly (butylene adipate-co-terephthalate) (PBAT): Extrusion

- compounding, cast extrusion and thermoforming of home compostable materials. Chin. J. Polym. Sci. **40** (10) (2022) 1269–86. http://dx.doi.org/10.1007/s10118-022-2734-0
- 7. Gui H., Zhao M.Y., Zhang S.Q., Yin R.Y. Active antioxidant packaging from essential oils incorporated polylactic acid/poly (butylene adipate-co-terephthalate)/thermoplastic starch for preserving straw mushroom, Foods, **11** (15) (2022) 2252. https://doi.org/10.3390/foods11152252
- 8. Yang X., Wang M., He C., Yang X., Duan G., Wang W. Preparation and properties of PLA/PBAT composites modified with different filler particles, Mater. Lett. **372** (2024) 136960. http://dx.doi.org/10.2139/ssrn.4811066
- 9. Giang N. V., Trung D. Q., Trung T. H., Huynh M. D., Minh N. Q. Study on the physical and mechanical properties and structure of the composite materials based on polypropylene and sodium dodecyl sulfate modified gypsum, Vietnam J. Chem. **52** (1) (2014) 101-106. https://doi.org/10.15625/4980
- 10. Ramos F. J. H. T. V., Mendes L. C. Recycled high-density polyethylene/gypsum composites: evaluation of the microscopic, thermal, flammability, and mechanical properties, Green Chem. Lett. Rev. **7** (2) (2014) 199–208. https://doi.org/10.1080/17518253.2014.924591
- 11. Lin W.-T., Korniejenko K., Mierzwiński D., Łach M., Cheng A., Lin K.-L. Feasibility Study of Waste Gypsum as a Full Replacement for Fine Aggregates of Controlled Low-Strength Material, Mater. Proc. **2023**, 13, 19. https://doi.org/10.3390/materproc2023013019
- 12. Jiang Z.-Y., Sun X.-P., Luo Y.-Q., Fu X.-L., Xu A., Bi Y.-Z. Recycling, reusing and environmental safety of industrial by-product gypsum in construction and building materials, Constr. Build. Mater. **432** (2024) 136609. http://dx.doi.org/10.1016/j.conbuildmat.2024.136609
- 13. Zhao Y. Q. Involvement of Gypsum (CaSO<sub>4</sub>·2H<sub>2</sub>O) in water Treatment Sludge Dewatering: A Potential Benefit in Disposal and Reuse, Sep. Sci. Technol. **41** (2006) 2785-2794. http://dx.doi.org/10.1080/01496390600785558
- 14. Denev Y. G., Denev G. D., & Popov A.N. Surface Modification of Phosphogypsum Used as Reinforcing Material in Polyethylene Composites, J. Elastomers Plast. **41** (2) (2009) 119–132. doi:10.1177/0095244308092436
- 15. Sun M., Sun Q., Zhang J., Sheng J. Modified phosphogypsum used as reinforcing material in composites, J. Reinf. Plast. Compos. **42** (3-4) (2023) 85-94. doi:10.1177/07316844221102935
- 16. Doleželová M., Krejsová J., Scheinherrová L., Keppert M., Vimmrová A. Investigation of environmentally friendly gypsum based composites with improved water resistance, J. Clean. Prod. **370** (2022) 133278. https://doi.org/10.1016/j.jclepro.2022.133278
- 17. Trung T. H., Huynh M. D., Cong D. V., Giang N. V. Mechanical properties and flame resistance of composite based on high density polyethylene/ethylene vinyl acetate blend and novel organically modified waste gypsum, Vietnam J. Sci. Technol. **56** (3B) (2018) 87-95. http://dx.doi.org/10.15625/2525-2518/56/3B/12915
- 18. Trung T. H., Huynh M. D., Mai T. T., Dat N. H., Linh N. T. D., Trang N. T. T., Hoang T., Giang N. V. Study on UV resistance of high-density polyethylene composite using waste gypsum, Vietnam Journal of Catalysis and Adsorption, **10** (1) (2021) 153-157. http://dx.doi.org/10.51316/jca.2021.112

- 19. Giang N. V. Study on the rheological, physico-mechanical and thermal properties of polyvinylchloride/waste-gypsum polymer composites, Vietnam J. Sci. Technol. **48** (2) (2012) 99-107. https://doi.org/10.15625/0866-708X/48/2/1131
- Giang N. V., Kang H.-J., Kang S.-Y., Jung D.-W., Ko J.-W., Hoang T., Tham D. Q., Kim M.-Y. Rheological Studies, Physico-Mechanical Properties, Thermal Properties and Morphology of PVC/Waste-Gypsum Composites, Compos. Technol. 27 (3) (2014) 115-121. http://dx.doi.org/10.7234/composres.2014.27.3.115
- 21. Murariu M., Ferreira A., Pluta M., Bonnaud L., Alexandre M., Dubois P. Polylactide (PLA)–CaSO<sub>4</sub> composites toughened with low molecular weight and polymeric ester-like plasticizers and related performances, Eur. Polym. J. **44** (11) (2008) 3842–3852. https://doi.org/10.1016/j.eurpolymj.2008.07.055
- 22. Huynh M. D., Trung T. H., Dat N. H., Giang N. V. The melting rheology, mechanical properties, thermal stability and morphology of polylactic acid/ethylene bis stearamide modified gypsum composite, Vietnam J. Chem. **58** (2) (2020) 251-255. https://doi.org/10.1002/vjch.201900187
- 23. Kong T. W., Kim I. T., Sinha T. K., Moon J., Kim D. H., Kim I., Na K., Kim M.-W., Kim H.-L., Hyeong T., Oh J. S. Effect of surface modifying sgents towards enhancing performance of waste gypsum based PBAT composite, Elastom. Compos. **55** (4) (2020) 347~353. http://doi.org/10.7473/EC.2020.55.4.347
- 24. Kong T. W., Kim I. T., Moon J., Sinha T. K., Kim D. H., Kim I., Na K., Choi K. W., Oh J. S. Comparing Waste Gypsum with CaCO<sub>3</sub> as Filler Towards Developing Low-cost PBAT Composites, Polym. Korea, **45** (1) (2021) 119-128. http://dx.doi.org/10.7317/pk.2021.45.1.119
- 25. 25. Ning N., Fu S., Zhang W., Chen F., Wang K., Deng H., Zhang Q., Fu Q. Realizing the enhancement of interfacial interaction in semicrystalline polymer/filler composites via interfacial crystallization, Prog. Polym. Sci. **37** (10) (2012) 1425-1455. https://doi.org/10.1016/j.progpolymsci.2011.12.005
- 26. Feng J., Venna S. R., Hopkinson D. P. Interactions at the interface of polymer matrix-filler particle composites, Polymer, **103** (2016) 189-195. https://doi.org/10.1016/j.polymer.2016.09.059
- 27. Olonisakin K., Fan M., Xiang Z., Ran L., Lin W., Zhang W., Wenbin Y. Key Improvements in Interfacial Adhesion and Dispersion of Fibers/Fillers in Polymer Matrix Composites; Focus on PLA Matrix Composites, Compos. Interfaces, **29** (10) (2021) 1071–1120. https://doi.org/10.1080/09276440.2021.1878441
- 28. Jang H. G., Jo J. Y., Jung U., Kim Y. N., Jung Y. C., Lee H., Lee D. C., Kim J. Revealing the filler–matrix interfacial interactions: Real-time observation with mechanoresponsive Spiropyran microbeads, ACS Appl. Mater. Interfaces. **16** (35) (2024) 46719-46727. http://dx.doi.org/10.1021/acsami.4c07977
- 29. Deshoulles Q., Gall M. L., Benali S., Raquez J-M., Dreanno C., et al. Hydrolytic degradation of biodegradable poly(butylene adipate-co-terephthalate) (PBAT) Towards an understanding of microplastics fragmentation, Polym. Degrad. Stab. **205** (2022) 110122. DOI 10.1016/j.polymdegradstab.2022.110122
- 30. Wang Y., Chen C., Li J., Huang J., Xiong L. Effect of carbodiimides on the compatibility and hydrolytic behavior of PLA/PBAT blends, Green Mater. **2024**, preprint. https://doi.org/10.1680/jgrma.24.00072.